

Supporting Information for Article:

Influence of Radioactivity on Surface Charging and Aggregation

Kinetics of Particles in the Atmosphere

Yong-ha Kim¹, Sotira Yiacoumi¹, Ida Lee², Joanna McFarlane³, Costas Tsouris^{1,3,*}

¹ Georgia Institute of Technology, Atlanta, Georgia 30332-0373, United States

² University of Tennessee, Knoxville, Tennessee 37996, United States

³ Oak Ridge National Laboratory, Oak Ridge, Tennessee 37831-6181, United States

Submitted for publication in

Environmental Science and Technology

Submitted in March 2013

Revised manuscript submitted in October and December 2013

Pages: 16 pages including cover sheet

Main contents: 1 text (Text S1), 6 figures (Figure S1-S6),

5 tables (Table S1-S5), and 10 equations (Equation S1-S10)

Experimental Section.

SSPM Measurement of Nonradioactive Materials Irradiated by ^{210}Po .

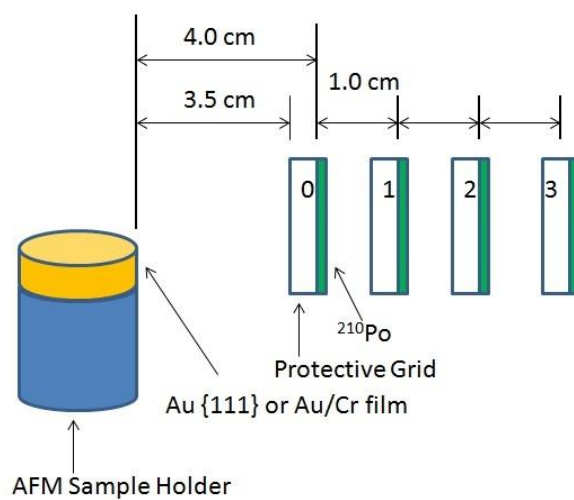


Figure S1. Experimental configuration showing the distance from the ^{210}Po radioactive source

SSPM Measurements of Radioactive Materials.

Table S1. Cs-137 Uptake into Mounted AMP/ZrHP Microspheres at Steady State

Coupon #	Averaged final count rate supernatant (cpm)	Difference in count rate (adsorbed ¹³⁷ Cs activity)	% uptake	Contact Beta (mR/h)	Contact Gamma (mR/h)
1	Not measured	Not applicable	Not applicable	0	0
2	61786	4598	6.93	226	0.5
3	129659	9523	6.84	414	1
4	180590	16712	8.47	516	1
5	237549	22900	8.79	942	2
6	313565	19279	5.79	7563	1.7
7	10910	1184	9.79	3.8	<0.5

Theoretical Section.

Collision Frequency and Collision Efficiency

$$V_A = -\frac{A}{6} \left[\frac{2r_i r_j}{s^2 - (r_i + r_j)^2} + \frac{2r_i r_j}{r^2 - (r_i - r_j)^2} + \ln \frac{s^2 - (r_i + r_j)^2}{s^2 - (r_i - r_j)^2} \right] \quad (\text{S1}) \quad (1, 2)$$

$$V_R = \frac{z_i z_j e^2}{4\pi\epsilon\epsilon_0 s} \quad (\text{S2}) \quad (2)$$

$$G^{-1} = 1 + \frac{2.6r_i r_j}{(r_i + r_j)^2} \left(\frac{r_i r_j}{(r_i + r_j)(s - r_i - r_j)} \right)^{0.5} + \left(\frac{r_i r_j}{(r_i + r_j)(s - r_i - r_j)} \right) \quad (\text{S3}) \quad (3)$$

In the equations above, μ is the fluid viscosity, s is the distance between the centers of the particles, A is the Hamaker constant, z is the number of electric charges of particles i and j , ϵ_0 is the permittivity of vacuum, and ϵ is the dielectric constant of the medium.

Simulation Scenario and Assumptions.

Table S2. Values of the parameters needed for the simulation (2, 4)

Parameters	m_+ (m ² /V/s)	m_- (m ² /V/s)	α (m ³ /s)	q (#/m ³ /s)	T (K)	A (J)
Values	1.14×10^{-4}	1.25×10^{-4}	1.6×10^{-12}	0	293	10^{-19}

RESULTS AND DISCUSSION

Surface charging by diffusion of positive and negative ions.

$$\frac{dC}{dt} = -KC \quad (\text{S4})$$

In the equations above, C is radioactivity and K is a first order constant.

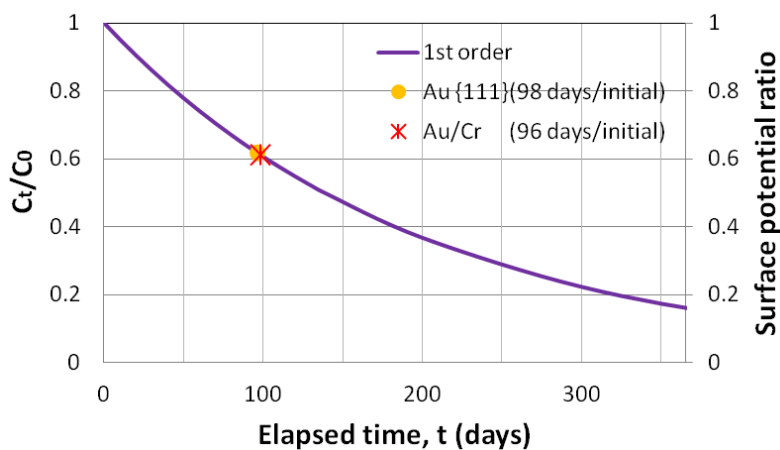


Figure S2. Surface potential of Au substrates and radioactivity of ^{210}Po .

Self-charging and Diffusion Charging of Surfaces.

$$I_{\alpha} = \frac{E_0}{2W_i} \quad (\text{S5}) \quad (5)$$

$$I_{\beta} = \frac{E_{\max}}{3W_i} \quad (\text{S6}) \quad (5)$$

$$R_{\alpha} = (1.24E_0(\text{MeV}) - 2.62) \times 10^{-2} \quad (\text{S7}) \quad (5)$$

In the equations above, I is number of ion-pairs produced per decay of alpha- or beta-emission, E_0 is alpha particle energy, E_{\max} is maximum beta particle energy, W_i mean energy required to form an ion pair (e.g. $W_{i,\text{air}} = 35$ eV), and R_{α} is the range of alpha particles.

Table S3. Ion-pairs produced per decay

Isotope	Decay type	E_{\max} (MeV)	I	R_{α} (cm)
^{210}Po	Alpha	5.3	7.6×10^4	3.952
^{137}Cs	Beta	0.512	5.0×10^3	-
^{131}I	Beta	0.81	7.7×10^3	-

Model Validation.

Mean number of charges.

$$\frac{N_j}{N_0} = \left(\frac{1}{\sqrt{2\pi}\sigma} \right) \exp\left(-\frac{(j-J)^2}{2\sigma^2}\right) \quad (\text{S8}) (4)$$

$$\sigma = \left[\frac{1}{2\lambda(r)} + y(r) \right]^{0.5} \quad (\text{S9}) (4)$$

Here, j is elementary charge, and σ is standard deviation of charge distribution.

Table S4. Quantitative comparison of two solutions to experimental data (6)

	Iterative solution (5)	Approximate solution (Eq 2)
Root mean square error	0.0213	0.0195

Population balance model.

$$n_{k,t} = \frac{n_{k,0}(0.5t\beta n_{k,0})^{k-1}}{(1+0.5t\beta n_{k,0})^{k+1}} \quad (\text{Eq S10}) (2)$$

Here, t is the aggregation time, β is the collision frequency function, n_k is the number concentration of particles.

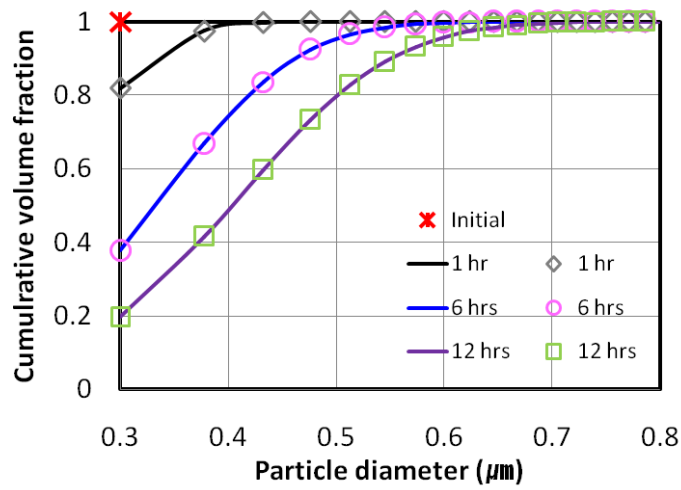


Figure S3. Comparisons of particle size distributions, plotted as cumulative volume fraction vs particle diameter, as obtained from the numerical solution (lines) of the population balance model and from the analytical solution (symbols) for initially monodisperse particle size distribution.

Aggregation Frequency of Radioactive Particles.

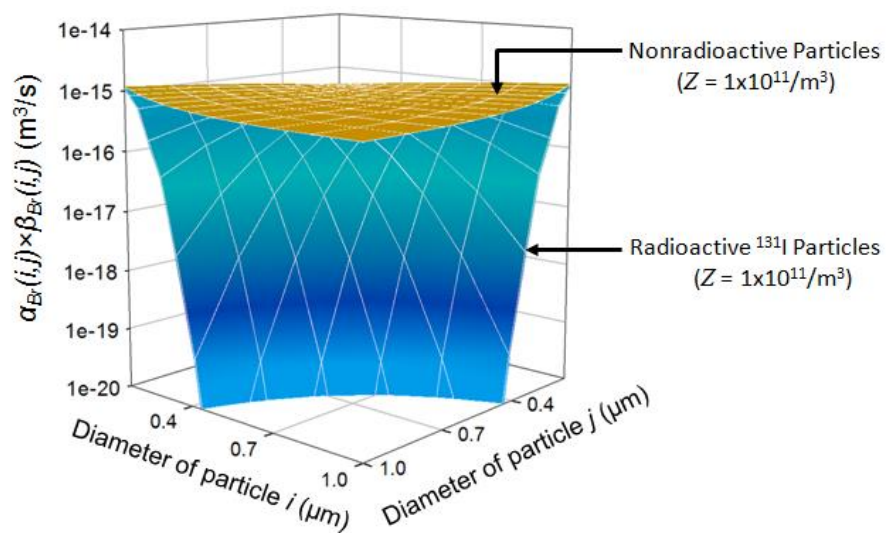


Figure S4. Aggregation frequency for (a) nonradioactive particles and (b) radioactive ^{131}I particles.

Aggregation of Radioactive Particles.

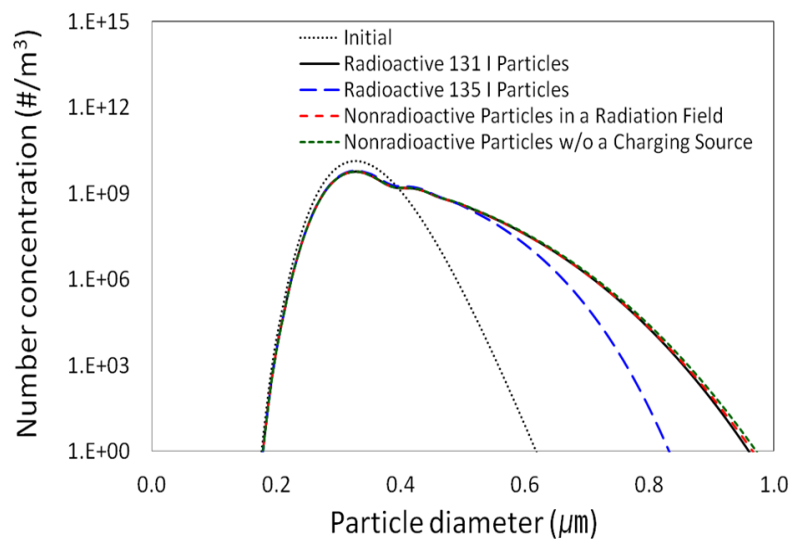


Figure S5. Aggregation of radioactive iodine particles, nonradioactive particles in a radiation field, and nonradioactive particles outside a radiation field for a log-normal initial distribution ($t = 6$ h; $Z = 10^{11}/\text{m}^3$).

Sensitivity analysis.

Text S1. Parameter selection for the sensitivity analysis

The initial particle size can influence λ and γ through Eq 2. As a part of a reactor safety program, Mulpuru et al. (7) investigated experimentally the characteristics of radioactive particles, which can be emitted during a postulated accident. The diameter of individual radioactive particles, generated from a hot nuclear fuel sample, was in a range of 0.1 to 0.3 μm and these particles were of spherical shape. Furthermore, monodispersed radioactive particles having a diameter of approximately 0.5 μm were used to investigate their potential inhalation hazard (8). Thus, a sensitivity analysis was carried out using particles having 0.1 to 0.5 μm diameter. The mean value of 0.3 μm was chosen as the standard.

The ion number concentration, which determines γ , depends on the particle concentration Z . There have been several experimental studies to investigate the effects of radioactivity on the charging and aggregation of a particle population (6, 8-10). In these studies, a wider range of Z was used in the experiment ($10^7 / \text{m}^3$ to $2 \times 10^7 / \text{m}^3$ or $2 \times 10^9 / \text{m}^3$ to $10^{12} / \text{m}^3$). Within a range of $10^{10} / \text{m}^3$ to $10^{12} / \text{m}^3$, Z can be similar to the background aerosol concentration. In the case of a nuclear event, background aerosols can easily interact with radionuclides or radioactive particles emitted from a radioactive source, and can also become radioactive. Thus, the values for Z used in this study were in the range of $10^{10} / \text{m}^3$ to $10^{12} / \text{m}^3$ and the mean value ($10^{11} / \text{m}^3$) was chosen as the standard.

The ion number concentration can also be influenced by the number of ion pairs produced per decay I . ^{131}I particles can emit beta particles having a high kinetic energy, which can dissociate the surrounding gas molecules along a linear path. The maximum kinetic energy of a single beta

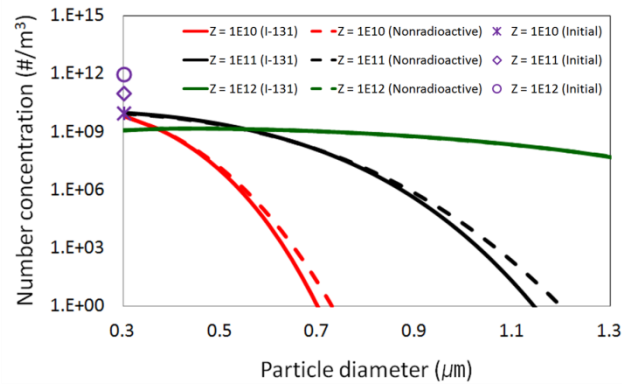
particle of ^{131}I is known to be 0.81 MeV, which corresponds to a maximum number of 7.7×10^3 ion pairs that can be produced per decay of ^{131}I (Table S4). However, the value for I can change as a function of the linear path length of the single beta particle. The value of the parameter I of beta-emitting radioactive particles having 0.96 MeV was approximately 55 in a transport line (1.5 cm in diameter, 40 cm in length) (8), while Eq (S6) gives a value of 9.1×10^3 for I . A value of 55 can be obtained by solving Eq (1) with the input data shown in (8, 11). The recent experiment of Gensdarmes et al. (6) more clearly showed the effects of the linear path on I . In that experiment, the maximum value for I of the beta emitting particles having 0.51 MeV was 4,395 in a cylinder tank (40 cm in diameter, 30 cm in height), but it was reduced to 52 in tubes (0.6 cm in diameter, 80 cm in height). These experimental results suggest that ^{131}I particles can have various I values similar to or lower than 7.7×10^3 . Thus, in this study, a sensitivity analysis was carried out with the maximum I value of ^{131}I and the values verified in the recent experiment (6) to analyze the effects of I on the radioactive particle aggregation.

The ion asymmetric parameter X can be defined as the ratio of positive and negative ion flux, but at steady state, it can be simplified to the ratio of the mobility of positive and negative ions (4). Under such condition, X can have the values: 0.737, 0.800, 0.912, and 1.000 (4-6, 8, 9, 11, 12). A value of 0.912 provided by Clement et al. (4) was chosen as the standard value.

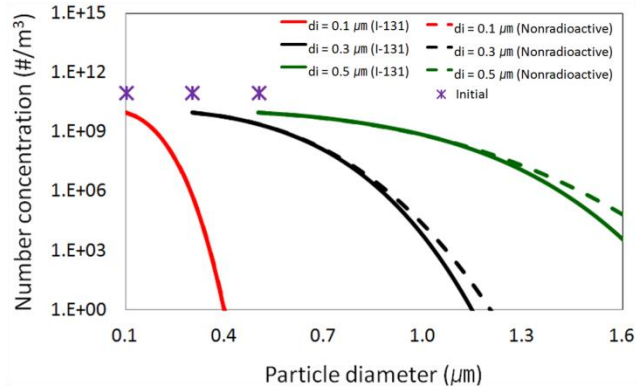
All variables used for the sensitivity analysis are now summarized in Table S5.

Table S5. Sensitivity analysis based on the major charging variables

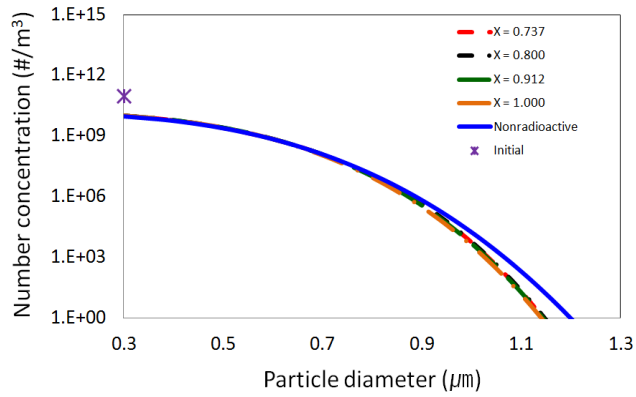
	$Z (/m^3)$	I	$d_i (\mu m)$	X
Standard values	10^{11}	7,700	0.3	0.912
Ranges of variables	$10^{10}/10^{11}/10^{12}$	52/ 4,395/ 7,700	0.1/ 0.3/ 0.5	0.737/0.800/ 0.912/ 1.000



(a)



(b)



(c)

Figure S6. Effects of charging parameters on particle aggregation: (a) particle concentration ($/m^3$), (b) initial size, (c) ion asymmetric parameter. ($t = 24$ h; Monodispersed initial condition with standard values)

References

- (1) Gauer, C.; Jia, Z.; Wu, H.; Morbidelli, M. Aggregation kinetics of coalescing polymer colloids. *Langmuir* **2009**, 25 (17), 9703-9713
- (2) Seinfeld, J.H.; Pandis, S.N. *Atmospheric Chemistry and Physics: From Air Pollution to Climate Change*; John Wiley and Sons: New York, 1998.
- (3) Alam, M.K. The effect of van der Waals and viscous forces on aerosol coagulation. *Aerosol Sci. Technol.* **1987**, 6 (1), 41-52.
- (4) Clement, C.F.; Clement, R.A.; Harrison, R.G. Charge distributions and coagulation of radioactive aerosols. *J. Aerosol Sci.* **1995**, 26 (8), 1207-1225.
- (5) Clement, C.F.; Harrison, R.G. The charging of radioactive aerosols. *J. Aerosol Sci.* **1992**, 23 (5), 481-504.
- (6) Gensdarmes, F.; Boulaud, D.; Renoux, A. Electrical charging of radioactive aerosols—comparison of the Clement–Harrison models with new experiments. *J. Aerosol Sci.* **2001**, 32 (12), 1437-1458.
- (7) Mulpuru, S.R.; Pellow, M.D.; Cox, D.S.; Hunt, C.E.L.; Barrand, R.D. Characteristics of radioactive aerosols generated from a hot nuclear fuel sample. *J. Aerosol Sci.* **1992**, 23 (S1), S827-S830.
- (8) Yeh, H.C.; Newton, G.J.; Raabe, O.G.; Boor, D.R. Self-charging of ^{198}Au -labeled monodisperse gold aerosols studied with a miniature electrical mobility spectrometer. *J. Aerosol Sci.* **1976**, 7 (3), 245-253.

- (9) Subramanian, V.; Kumar, A.; Baskaran, R.; Misra, J.; Venkatraman, B. An experimental study on the charging of non-radioactive aerosols with and without the presence of gamma radiation. *J. Aerosol Sci.* **2012**, *52*, 98-108.
- (10) Rosinski, J.; Werle, D.; Nagamoto, C.T. Coagulation and scavenging of radioactive aerosols. *J. Colloid Sci.* **1962**, *17* (8), 703-716.
- (11) Reed, L.D.; Jordan, H.; Gieseke, J.A. Charging of radioactive aerosols. *J. Aerosol Sci.* **1977**, *8* (6), 457-463.
- (12) Adachi, M.; Kousaka, Y.; Okuyama, K. Unipolar and bipolar diffusion charging of ultrafine aerosol particles. *J. Aerosol Sci.* **1985**, *16* (2), 109-123.